Macromolecular Research, Vol. 17, No. 11, pp 894-900 (2009)

Charge Carrier Photogeneration and Hole Transport Properties of Blends of a π-Conjugated Polymer and an Organic-Inorganic Hybrid Material

Jungwook Han, Jongdeok An, R. N. Jana, Kyungna Jung, Junghwan Do, Seungmoon Pyo, and Chan Im*

Department of Chemistry, Konkuk University, Seoul 143-701, Korea

Received March 25, 2009; Revised April 25, 2009; Accepted May 5, 2009

Abstract: This study examined the charge carrier photogeneration and hole transport properties of blends of poly (9-vinylcarbazole) (PVK), a π-conjugated polymer, with different weight proportions (0~29.4 wt%) of (PEA)-$VOPO_4 \cdot H_2O$ (PEA: phenethylammonium cation), a novel organic-inorganic hybrid material, using IR, UV-Vis, and energy dispersive spectroscopy (EDS), thermogravimetric analysis (TGA), steady state photocurrent (SSPC) measurement, and atomic force microscopy (AFM). The SSPC measurements showed that the photocurrent of PVK was reduced by approximately three orders of magnitude by the incorporation of a small amount (~12.5 wt%) of (PEA) $VOPO_4 \cdot H_2O$, suggesting that hole transport occurred through the PVK carbazole groups, whereas a reverse trend was observed at high proportions (>12.5 wt%) of (PEA)$VOPO_4 \cdot H_2O$, suggesting that transport occurred via (PEA)$VOPO_4 \cdot H_2O$ molecules. The transition to a trap-controlled hopping mechanism was explained by the difference in ionization potential and electron affinity of the two compounds as well as the formation of charge percolation threshold pathways.

Keywords: charge carrier photogeneration, hole transport, conjugated polymer, hybrid material, vanadium phosphate, photocurrent.

Introduction

Recently, polymer-based photovoltaic materials have become more attractive for their advantages of low cost, light weight and easy processability.[1-5] However, their limited exciton diffusion length, low electrical conductivity, low charge-carrier mobility, narrow absorption spectrum and low chemical and thermal stability have protected them from their practical uses. In order to overcome these problems, a broad range of materials are currently being developed using different techniques, e.g., dye-sensitization of photoelectrochemical materials,[6-9] introduction of heterojunction in bulk composites (polymer/fullerene),[10,11] and development of hybrid materials (organic-inorganic),[12-17] etc.. To get good organic photovoltaic (OPV) material, there should be easy charge carrier photogeneration, facilitated by doping with either high electron affinity or very low oxidation potential materials (dopants), and fast charge transport to the respective electrodes.[18]

In our present study we have chosen poly(9-vinylcarbazole) (PVK) as an active polymeric material because it is being used as one of the most popular OPV materials during last decade. There are several reports on its charge carrier photogeneration and hole transport properties.[19-24] In general, during charge carrier photogeneration, an exciton can dissociate one of its charge to the dopant and leave the other in the polymer. It is found that in presence of various charge acceptors, both the charge carriers are mobile and are collected by the electrodes according to polarities of the applied electric fields. Thus for a high efficient OPV material, every exciton should reach the dopant, and the photogenerated electron-hole pairs should dissociate into free carriers rather than recombining geminately.[25,26] For the PVK based compounds, the hole transport phenomena occurs by hopping mechanism between adjacent carbazole chromophores pendant to the main hydrocarbon chain.[27,28] Thus electroabsorption measurements of the complexes of PVK with 2,4,7-trinitro-9-fluorenone (TNF) show that electron transport dominates in TNF molecules, while hole transport is favorable through PVK molecules.[29] Pai *et al.*[30] investigated hole transport of PVK doped with *N,N'*-diphenyl-*N,N'*-bis(3-methylphenyl)-(1,1'-biphenyl)-4,4'-diamine (TPD) and found that the hole mobilities in PVK blend were reduced by the incorporation of small amount of TPD whereas, at its high concentrations, the mobilities are higher in TPD than PVK suggesting that at low concentration, the transport proceeds through PVK carbazole groups whereas the TPD molecules remain as trap but at high concentrations, transport occurs via the TPD molecules. Generally, the trap may be due to either small molecular defect, impu-

*Corresponding Author. E-mail: chanim@konkuk.ac.kr

rity in monomer units incorporated in the polymer chain, or localized regions of compression introduced by polymer chain entanglements.[31,32] Here, we report the new organic-inorganic hybrid material (PEA)$VOPO_4 \cdot H_2O$ (PEA: phenethylammonium cation) which is used in different concentrations with PVK to study its effect on charge carrier photogeneration and hole transport mechanism of the blends.

Experimental

Materials. All chemicals during this work were of reagent grade and used as received from commercial sources without further purification. Poly(9-vinylcarbazole) (PVK) with M_w 1,100,000 g/mol, refractive index ($\mu^{20}{}_D$) 1.683, T_g 220 °C, density 1.2 g/mL; vanadium pentaoxide (V_2O_5), with mp 690 °C, density 3.35 g/mL and purity ~99.6%; phosphoric acid (H_3PO_4) with density 1.685 g/mL, 85 wt% in H_2O; phenethylamine (PEA) with bp 197-200 °C, refractive index ($\mu^{20}{}_D$) 1.533, density 0.962 g/mL, and purity ~99.0%, were purchased from Aldrich Co., USA.

Hydrothermal Synthesis of a New Hybrid Material (PEA)$VOPO_4 \cdot H_2O$. Hydrothermal reactions were carried out in 23 mL capacity Teflon-lined stainless steel Parr hydrothermal reaction vessels at 150 °C for 2 days. V_2O_5 (0.090 g, 0.5 mmol), H_3PO_4 (0.07 mL, 1.0 mmol), phenethylamine (0.38 mL, 3.0 mmol), and H_2O (5 mL) were allowed to react. The solution pH values before and after the reaction were ~2.5 and ~3.0, respectively. The product was filtered and washed with distilled water. The tiny dark blue platy crystals were found with the unidentified black powder. A yield of the product, (PEA)$VOPO_4 \cdot H_2O$ was 62%, based on vanadium. The products are stable in air and water. The products were insoluble in common polar and non-polar solvents.

Preparation of the Blends and Device Fabrication. A constant concentration of 2 wt% of five different solutions were made in chlorobenzene (Aldrich, USA, purity ≥99%) from the blends of PVK with 0, 5.8, 12.5, 20.6 and 29.4 wt% of (PEA)$VOPO_4 \cdot H_2O$. The solution was stirred at 500 rpm for 12 h to get rid of possible polymer chains entanglement and syringe filtered (pore size: 0.22 μm) before making a thin film by drop-casting method. The film thickness was maintained by using a constant volume of the solution dropped from a micropipette on to the ITO surface. Then the film was dried for 1 h at room temperature (25 °C) prior Al electrode deposition by a conventional thermal evaporator (JBS International, Korea) under vacuum maintained at about 10^{-6}~10^{-7} Torr. The film thickness was approximately 100 nm measured using thickness/rate monitor, SQM-160 (Sigma Instruments, USA). For steady-state photocurrent measurement, single layer devices with an ITO/blend/Al sandwich structure were prepared. Aluminum top electrodes of 9 mm^2 active area were evaporated onto the blend films.

Characterization. Thermogravimetric analysis (TGA) was carried out in N_2 at a heating rate of 5 °C/min, using a high-resolution Perkin-Elmer TGA7 Thermal Analyzer. Infrared spectrum was recorded on a Hartmann & Braun BOMEM FTIR spectrometer within a range of 400~4000 cm^{-1} using the KBr pellet method. Semiquantitative analysis of the compound was performed with JEOL JSM-5200 scanning electron microscope (SEM) equipped with an EDAX Genesis energy dispersive spectroscopy (EDS) detector. For UV-Vis spectra of the solutions, a commercial UV-Vis spectrophotometer (Cary 100, Varian Inc., USA) and for photocurrent measurement, a temperature-controlled vacuum chamber with a combination of a monochromator and a xenon arc lamp as a light source, were used. Photocurrent signals were detected with a lock-in amplifier (Model 7260, EG&G Instrument), which was connected to a chopper operated at a frequency of 20~40 Hz. For phase morphology, atomic force microscopy (AFM) (Seiko SPA 300HV, Japan) and for thickness measurement, a surface profiler, Dektak (Veeco, USA) were used.

Results and Discussion

Characterizations of (PEA)$VOPO_4 \cdot H_2O$. The title compound can be well characterized by energy dispersive spectroscopy, infrared spectroscopy, and thermogravimetric analysis although the products obtained from the hydrothermal reactions were too small to structurally analyze with the use of a single crystal X-ray diffractometer. The expected structure of the compound is also suggested based on the previously reported phases containing unique $VOPO_4$ layers.

EDS analysis of the dark blue platy crystals gave an average stoichiometric ratio of V:P=1:1, and the blue color of the crystals strongly support the oxidation state of V(IV) due to the characteristic vanadyl group, V=O in the structure. The IR spectrum for (PEA)$VOPO_4 \cdot H_2O$ exhibit the characteristic features of the V-O, V=O, and P-O at 1141, 1090, 1031, 988, 934, 876, 817, 746, 680, 614, 514, and 437 cm^{-1}. The stretching and bending vibrations for C-C, C-N, C-H, N-H, and O-H are observed at 3404, 3028, 1619, 1496, and 1454 cm^{-1}, respectively. The thermal decomposition of (PEA)$VOPO_4 \cdot H_2O$ occurs in several steps from ~110 to ~500 °C (Figure 1). The weight loss process below ~440 °C is due to the loss of the phenethylamine and water molecules (weight loss calcd 49.0%, exptl 48.4%). At this temperature, a weight increase is observed corresponding to the oxidation of V^{4+} to V^{5+} due to traces of oxygen in the balance. Assuming that the residue above 500 °C corresponds to $\frac{1}{2}V_2O_5$ and $\frac{1}{2}P_2O_5$, then the overall observed weight loss of 45.6% is in good agreement with that calculated value (46.4%) for the composition (PEA)$VOPO_4 \cdot H_2O$. The final product after heat treatment is glassy residue and cannot be identified by Powder-XRD. Based on the formula and other known vanadium phosphate structures, one most probable

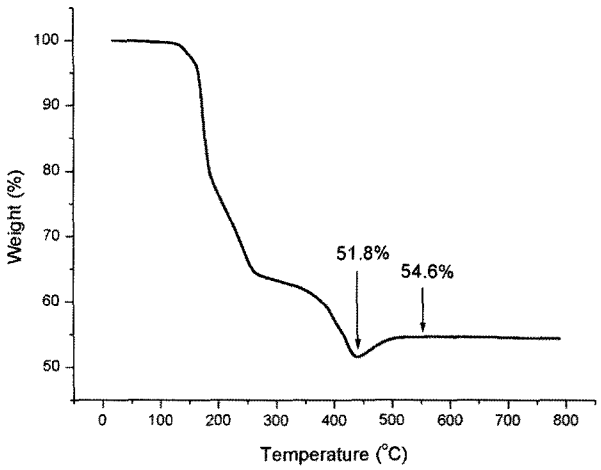

Figure 1. TG curve for (PEA) $VOPO_4 \cdot H_2O$.

structure of the compound (PEA) $VOPO_4 \cdot H_2O$ is the construction of the $VOPO_4$ layers of $V(IV)O_5$ square pyramids and PO_4 tetrahedra with PEA^+ cations and water molecules between the layers found in $(NH_4)VOPO_4 \cdot 1.5H_2O$.[33]

The other feasible structure could be the $VOPO_4 \cdot H_2O$ layered structure of $V(IV)O_5(H_2O)$ octahedra and PO_4 tetrahedra and interlayer PEA^+ cations as found in $(NH_4)_{0.5}VOPO_4 \cdot 1.5H_2O$.[33] The arrangement and orientation of PEA^+ cations is expected to possess a bilayer configuration that the hydrophilic $-NH_3$ parts points $VOPO_4$ or $VOPO_4 \cdot H_2O$ inorganic layers. Examples containing PEA^+ cations and metal chlorides, $(PEA)_2CuCl_4$ and $(PEA)_2PbCl_4$ strongly support the bilayer arrangement of PEA^+ between the layers.[34] The structure of (PEA) $VOPO_4 \cdot H_2O$ is also believed to be closely related to the tetragonal layer structure of $VOPO_4 \cdot 2H_2O$ and other layered mixed valence vanadium phosphate hydrates containing interlayer metal cations and (piperazineH_2) $VOPO_4$ Figure 2.

Effect of (PEA)$VOPO_4 \cdot H_2O$ on Optical Properties of PVK. The effect of (PEA)$VOPO_4 \cdot H_2O$ on optical properties of PVK was observed with the help of UV-Vis spectroscopy. Here both the neat PVK and the blend with 29.4 wt% (PEA)$VOPO_4 \cdot H_2O$ show sharp absorption peaks at 330 nm (3.75 eV) and 350 nm (3.60 eV) (Figure 3), consistent with the absorptions due to the presence of carbazole group.[35] From the figure it is also clear that PVK becomes transparent with respect to the UV-Vis spectra at a longer wave length than 360 nm, however, the absorption spectrum for the PVK:(PEA)$VOPO_4 \cdot H_2O$ blend shows a shoulder starting from 360 up to 500 nm. Thus for the blend the higher absorption in the shoulder zone with longer wavelength i.e., lower energy may be due to π-π^* transition between the aromatic rings of PVK and intercalated ammonium salt. Similar observation was found for $[Os(phen)_2(dppene)]^{2+}$/PVK complex,[36] however, the transition was mainly to due metal-to-ligand charge transfer of the hybrid material. The

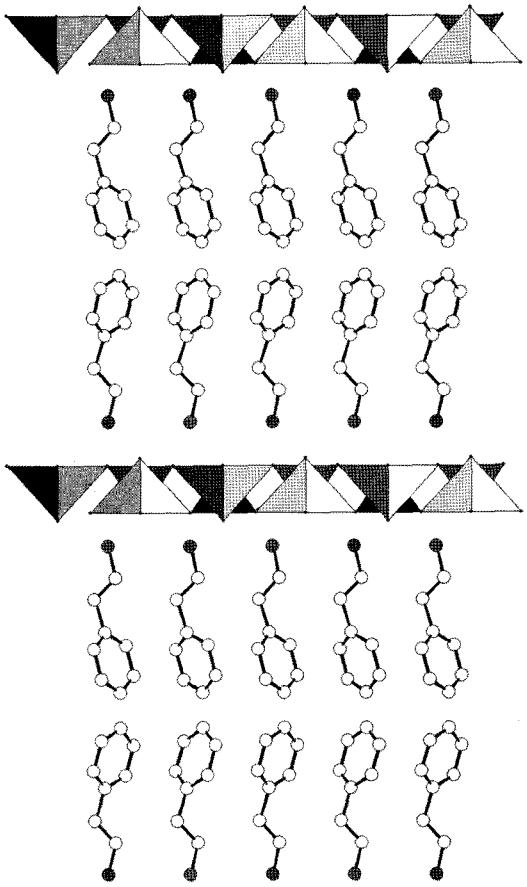

Figure 2. A hypothetical model of (PEA)$VOPO_4 \cdot H_2O$. View of stacking of $VOPO_4$ layers - $V(IV)O_5$ square pyramids and PO_4 tetrahedra - and bilayered PEA^+ cations.

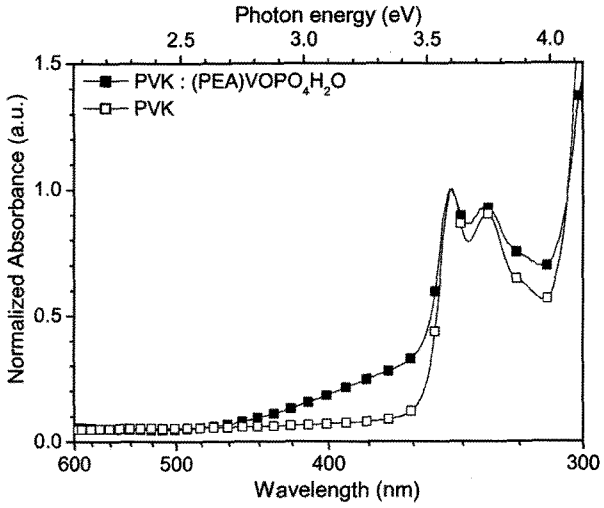

Figure 3. UV-Vis absorption spectra of PVK and PVK: (PEA)$VOPO_4 \cdot H_2O$ blend (29.4 wt% (PEA)$VOPO_4 \cdot H_2O$) films.

color changing from white of PVK to light blue of the blends suggests successful intercalation of the ammonium salt into the vanadium oxide.

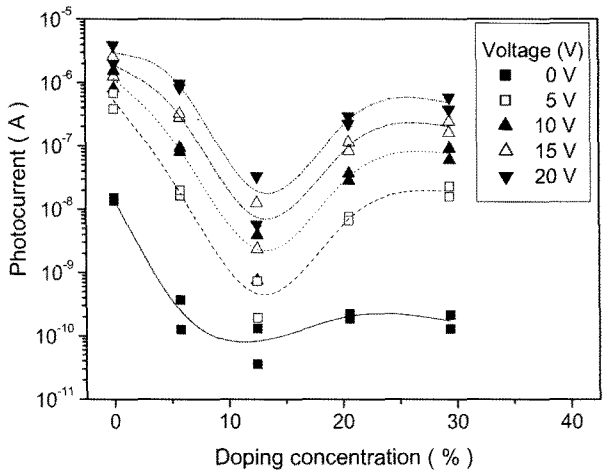

Figure 4. (PEA)$VOPO_4 \cdot H_2O$ doping concentration dependant photocurrent.

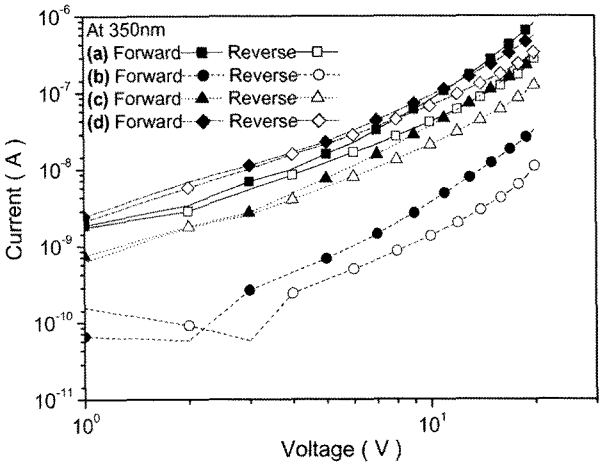

Figure 5. Variation of photocurrent with bias voltage at 350 nm irradiation of ITO/PVK:(PEA)$VOPO_4 \cdot H_2O$/Al device at room temperature with different doping concentrations of (PEA)$VOPO_4 \cdot H_2O$ (a) 5.8, (b) 12.5, (c) 20.6, and (d) 29.4 wt%.

Effect of (PEA)$VOPO_4 \cdot H_2O$ on Charge Carrier Photogeneration of PVK. Figure 4 shows the variation of photocurrent with doping concentration of (PEA)$VOPO_4 \cdot H_2O$ in the blends at different applied forward bias voltages (0~20 V). It is found that photocurrent measured at any constant applied voltage decreases initially with increasing doping concentration (up to 12.5 wt%) of (PEA)$VOPO_4 \cdot H_2O$ but afterwards, it shows a reverse trend. For instance, the photocurrent measured at 5 V of forward bias voltage, of PVK and the blend, containing 12.5 wt% (PEA)$VOPO_4 \cdot H_2O$ are about 5.2×10^{-7} and 4.6×10^{-10} A, respectively (Figure 4). Thus the photocurrent is reduced by about three orders of magnitude. This is because at low wt proportion of (PEA) $VOPO_4 \cdot H_2O$ (<12.5 wt%), the charge generated from exciton dissociation remains in the hybrid molecules as trap thus showing lower photocurrent whereas at high proportion (>12.5 wt%), the improved photocurrent may be due to greater exciton dissociation at extended interfacial area and reduced recombination due to better charge separation at the heterojunctions.[37]

We have also measured photocurrent at different bias polarity to get an idea about the charge transport direction and to compare between extrinsic and intrinsic photogeneration trends (Figure 5). And it was found that the photocurrent generated for all the blends with a forward bias becomes higher than that of their corresponding backward bias as reported earlier.[38] Again as observed from Figure 3 for UV spectra there are two major peaks at 330 and 350 nm, so we tried to observe the trend of photocurrent with forward and reverse bias at a constant irradiation (e.g., 350 nm).

Here also we can see that the photocurrent continuously increases with increasing forward bias but decreases with reverse voltage (Figure 6). This is because the electron and hole photoexcited by π-π^* transition in the conducting polymer can be transferred to (PEA) $VOPO_4 \cdot H_2O$ polymer pref-

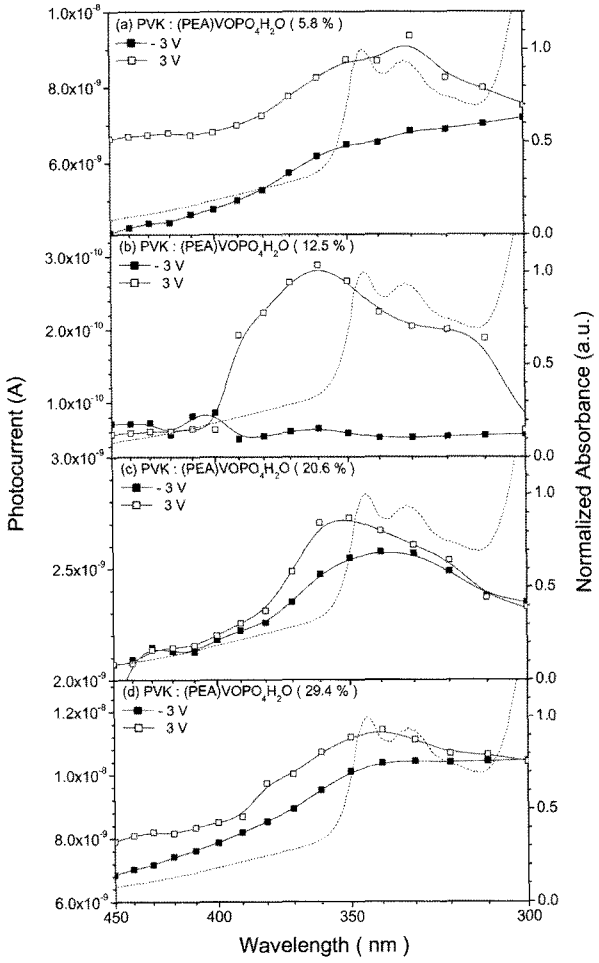

Figure 6. Variation of photocurrent with excitation wavelength for different blends (a) 5.8, (b) 12.5, (c) 20.6, and (d) 29.4 wt% of (PEA)$VOPO_4 \cdot H_2O$.

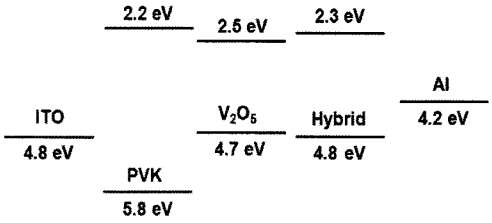

Figure 7. Schematic band diagram of PVK, vanadium oxide and hybrid material ((PEA)$VOPO_4 \cdot H_2O$).

erentially. Thus the charge transfer directions are in agreement with the forward bias direction and hence, by applying forward bias, the photoinduced charge transfer is activated and accelerated, resulting in the large photocurrent.

On the other hand, in the case of backward bias, the photoinduced charge transfer is not enhanced because the electric field direction is inverse to the charge transfer direction from PVK to (PEA)$VOPO_4 \cdot H_2O$, resulting in the small photocurrent. There is a similar report of photoinduced effect on poly(2-methoxy-5-(2′-ethyl-hexyloxy)-*p*-phenylene vinylene)/C_{60} system.[39]

Effect of (PEA)$VOPO_4 \cdot H_2O$ on Hole Transport Properties. For (PEA)$VOPO_4 \cdot H_2O$ the band gap is 2.5 eV which is smaller than that of PVK (3.6 eV) (Figure 7). Also, for V_2O_5, the HOMO and LUMO have potential energy level of 2.5 and 4.7 eV, respectively.[40] The scheme for hopping mechanism at low and high loading of (PEA)$VOPO_4 \cdot H_2O$ is shown in Figure 8.

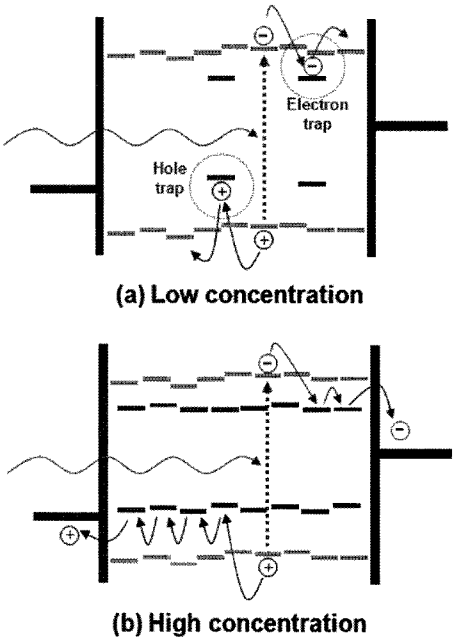

Figure 8. Scheme of hole/electron trap effect of PVK doped with (a) low concentration (<12.5 wt%), and (b) high concentration (>12.5 wt%) of (PEA)$VOPO_4 \cdot H_2O$.

It is speculated that the charge transfer from the LUMO potential energy level of PVK is mainly due to photo-induced charge transfer.

Typically charge transfer depends on ionization potential of donor, electron affinity of acceptor, and coulombic energy between separated counter ions.[41] Hole-transporter in the blends with (PEA)$VOPO_4 \cdot H_2O$ results in efficient devices due to rapid charge transfer and the existence of charge percolation pathways caused by the presence of aggregated (PEA)$VOPO_4 \cdot H_2O$. As the size of the aggregates affects largely the charge transport phenomena, it is highly dependent upon device fabrication and blend ratio.[42] Thus the best device performance does not necessarily correlate with the highly excited state lifetime, but also on morphological differences, such as charge pathways that enable efficient charge carrier transport.

Effect of (PEA)$VOPO_4 \cdot H_2O$ on Phase Morphology of the Blend. We have studied the morphological changes in the blends with the incorporation of the hybrid material ((PEA)$VOPO_4 \cdot H_2O$) and tried to correlate with the device performance. As discussed earlier the performance of an OPV device is severely limited by poor free charge carrier generation and charge carrier transport due to high rate of exciton recombination and low charge carrier mobilities in disordered polymer solids. This challenge can be partially overcome through the use of blend heterojunctions[43] as this type morphology offers multiple exciton dissociation sites and forming separated charge carrier pathways, thus limiting exciton recombination.[44] The phase morphology can be controlled by several parameters during the film formation and subsequent treatments.

The most significant factors which influence on the morphology in the blends are the film preparation method, i.e. either spin casting or drop casting, the blend composition, the solution concentration, the controlled phase separation and crystallization induced by thermal annealing, and finally the chemical structure of the materials. Finely phase-separated polymer blend is necessary to overcome the limited exciton diffusion length generally observed in the organic semiconductors.[45] The typical distances that these photo-excitations can travel within the material are around 10 nm. From the micrographs of PVK (Figure 9(a)) and the blend with low concentration of (PEA)$VOPO_4 \cdot H_2O$ (Figure 9(b)), it is clear that both the exposed surfaces of the samples have almost the same roughness. Thus at low concentration (<12.5 wt%) of (PEA)$VOPO_4 \cdot H_2O$, the particles are uniformly dispersed into the PVK matrix but at high concentration (>12.5 wt%) the (PEA)$VOPO_4 \cdot H_2O$ molecules may form few agglomerates showing numerous hills and valleys (Figure 9(c)) which help in formation of charge transporting pathways. Thus in an efficient bulk heterojunction the scale of phase separation is therefore closely related to the respective exciton diffusion lengths of the two materials involved. If the excitons reach the donor/acceptor interface, the

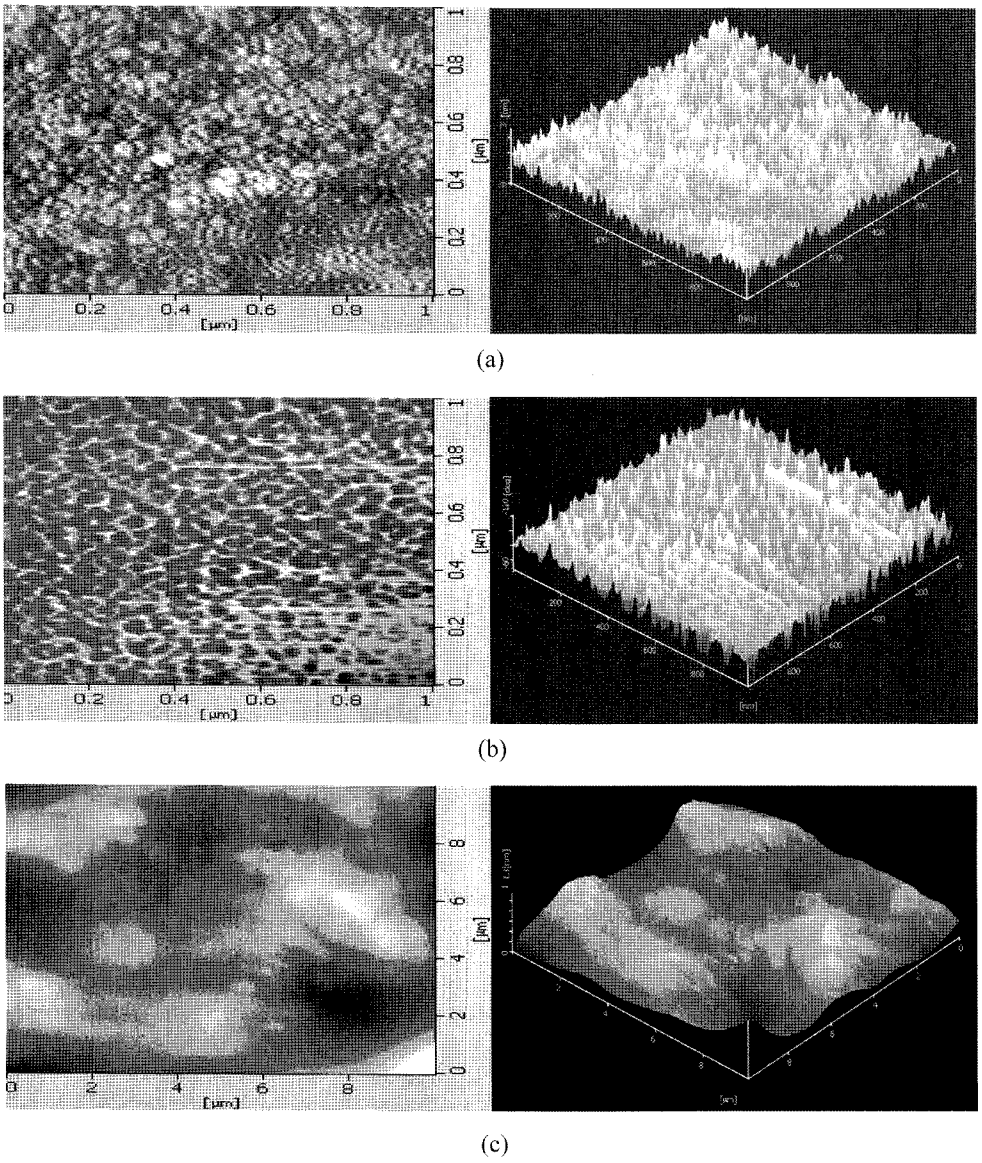

Figure 9. Phase morphology of PVK:(PEA)$VOPO_4 \cdot H_2O$ blends with different proportion of (PEA)$VOPO_4 \cdot H_2O$ (a) 0, (b) 5.8 and (c) 29.6 wt%.

charge transfer results in the exciton dissociation. After the charges have been separated they require percolated pathways to the respective charge extracting electrodes in order to supply an external direct current. Thus an effective charge transport relies on the development of a suitable morphology interpenetrating phase structures within the blend systems.

Conclusions

The exciton dissociation and hole transport properties of the various PVK:(PEA)$VOPO_4 \cdot H_2O$ blends studied by SSPC action spectroscopy, reveal that the photocurrent of PVK was reduced by three orders of magnitude by the incorporation of small amount (up to 12.5 wt%) of (PEA)$VOPO_4 \cdot H_2O$, suggesting that the hole transport occurred through the PVK carbazole groups, whereas at high proportion of (PEA)$VOPO_4 \cdot H_2O$ (>12.5 wt%), a reverse trend was observed, suggesting that the transport occurred via (PEA)$VOPO_4 \cdot H_2O$ molecules. The hopping mechanism was explained by the difference in ionization potential and electron affinity of the two compounds and the formation of charge percolation threshold pathways. The observed results are in agreement with the discrete phase morphology of the blends as studied by AFM.

Acknowledgements. This work was supported by the Korea Research Foundation Grant funded by the Korean

Government (MOEHRD, Basic Research Promotion Fund) (KRF-2006-312-C00571), Seoul R&BD Program (WR090671) and 2008 KU Brain Pool Program of Konkuk University, Korea.

References

(1) P. Suresh, P. Balaraju, S. K. Sharma, M. S. Roy, and G. D. Sharma, *Sol. Energ. Mater. Sol.Cell.*, **92**, 900 (2008).
(2) S. Gunes, D. Baran, G. Gunbas, F. Ozyurt, A. Fuchsbauer, N. S. Sariciftci, and L. Toppare, *Sol. Energ. Mater. Sol. Cell.*, **92**, 1162 (2008).
(3) Z. Liu, Q. Liu, Y. Huang, Y. Ma, S. Yin, X. Zhang, W. Sun, and Y. Chen, *Adv. Mater.*, **20**, 3924 (2008).
(4) G. Li, V. Shrotriya, J. Huang, Y. Yao, T. Moriarty, K. Emery, and Y. Yang, *Nature Materials*, **4**, 864 (2005).
(5) H. K. Kim, S. G. Roh, K. S. Hong, J. W. Ka, N. S. Baek, J. B. Oh, M. K. Nah, Y. H. Cha, and J. Ko, *Macromol. Res.*, **11**, 133 (2003).
(6) E. Stathatos, P. Lianos, V. Jovanovski, and B. Orel, *J. Photochem. Photobiol. A: Chem.*, **169**, 57 (2005).
(7) K. Tennakone, G. K. R. Senadeera, V. P. S. Perera, I. R. M. Kottegoda, and L. A. A. De Silva, *Chem. Mater.*, **11**, 2474 (1999).
(8) R. S. Mane, J. Chang, D. Hama, B. N. Pawar, T. Ganesh, B. W. Cho, J. K. Lee, and S. H. Han, *Curr. Appl. Phys.*, **9**, 87 (2009).
(9) H. J. Shim, D. W. Kim, C. Lee, and Y. Kang, *Macromol. Res.*, **16**, 424 (2008).
(10) H. Jin, Y. Hou, F. Teng, P. Kopola, M. Tuomikoski, and A. Maaninen, *Sol. Energ. Mater. Sol. Cell.*, **93**, 289 (2009).
(11) S. Cho, J. K. Lee, J. S. Moon, J. Yuen, K. Lee, and A. J. Heeger, *Org. Elec.*, **9**, 1107 (2008).
(12) C. Girotto, D. Cheyns, T. Aernouts, F. Banishoeib, L. Lutsen, T. J. Cleij, D. Vanderzande, J. Genoe, J. Poortmans, and P. Heremans, *Org. Elec.*, **9**, 740 (2008).
(13) M. Wang, Y. Lian, and X. Wang, *Curr. Appl. Phys.*, **9**, 189 (2009).
(14) J. C. Lee, W. Lee, S. H. Han, T. G. Kim, and Y. M. Sung, *Electrochem. Comm.*, **11**, 231 (2009).
(15) C. W. Hsu, L. Wanga, and W. F. Su, *J. Colloid Interf. Sci.*, **329**, 182 (2009).
(16) Z. J. Wang, S. C. Qu, X. B. Zeng, J. P. Liu, C. S. Zhang, F. R. Tan, L. Jin, and Z. G. Wang, *Appl. Surf. Sci.*, **255**, 1916 (2008).
(17) H. J. Chen, L. Y. Wang, and W. Y. Chiu, *Mat. Chem. Phys.*, **112**, 551 (2008).
(18) S. H. Jin, J. M. Shim, S. J. Jung, S. C. Kim, B. V. K. Naidu, W. S. Shi, Y. S. Gal, J. W. Lee, J. H. Kim, and J. K. Lee, *Macromol. Res.*, **14**, 524 (2006).
(19) J. C. Ribierre, T. Aoyama, T. Muto, Y. Imase, and T. Wada, *Org. Elec.*, **9**, 396 (2008).
(20) D. P. West, M. D. Rahn, C. Im, and H. Bassler, *Chem. Phys. Lett.*, **326**, 407 (2000).
(21) I. Głowacki, J. Jung, and J. Ulanski, *Synth. Met.*, **109**, 143 (2000).
(22) J. G. Winiarz, L. Zhang, M. Lal, C. S. Friend, and P. N. Prasad, *Chem. Phys.*, **245**, 417 (1999).
(23) K. S. Narayan and G. L. Murthy, *Chem. Phys. Lett.*, **276**, 441 (1997).
(24) M. Y. Song, K. J. Kim, and D. Y. Kim, *Macromol. Res.*, **14**, 630 (2006).
(25) S. Q. Min, H. Y. Bing, L. Yan, F. Z. Hui, and L. X. Jun, *Chin. Phys. Lett.*, **26**, 017202 (2009).
(26) S. E. Watkins, K. L. Chan, S. Y. Cho, N. R. Evans, A. C. Grimsdale, A. B. Holmes, C. S. K. Mak, A. J. Sandee, and C. K. Williams, *Macromol. Res.*, **15**, 129(2007).
(27) P. M. Borsenberger and D. S. Weiss, *Organic Photoreceptors for Xerography*, Marcel Dekker Inc., New York, 1998, p 459.
(28) H. Hoegl, G. Barchietto, and D. Tar, *J. Photochem. Photobiol.*, **16**, 335 (1972).
(29) G. Weiser, *J. Appl. Phys.*, **43**, 5028 (1972).
(30) D. M. Pai, J. F. Yanus, and M. Stolka, *J. Phys. Chem.*, **88**, 4714 (1984).
(31) P. J. Reucroft and K. Takahashi, *J. Non Cryst. Solids*, **17**, 71 (1975).
(32) B. Reimer and H. Bässler, *Phys. Status Solidi(a)*, **51**, 445 (1979).
(33) J. Do, R. P. Bontchev, and A. J. Jacobson, *Inorg. Chem.*, **39**, 3230 (2000).
(34) (a) R. D. Willett, *Acta Crystallogr.*, **C46**, 565 (1990). (b) D. B. Mitzi, *J. Solid State Chem.*, **145**, 695 (1999).
(35) J. H. Park, O. O. Park, J. Kim, J. W. Yu, J. K. Kim, and Y. C. Kim, *Curr. Appl. Phys.*, **4**, 659 (2004).
(36) D. Pentlehner, I. Grau, and H. Yersin, *Chem. Phys. Lett.*, **455**, 72 (2008).
(37) V. Chasteen, J. O. Harter, G. Rumbles, J. C. Scott, Y. Nakazawa, M. Jones, H.-H Hörhold, H. Tillman, and S. A. Carter, *J. Appl. Phys.*, **99**, 033709 (2006).
(38) C. Im, E. V. Emelianova, and H. Bässler, *J. Chem. Phys.*, **117**, 2961 (2002).
(39) N. S. Sariciftci, D. Braun, C. Zhang, V. Srdranov, A. J. Heeger, and F. Wudl, *Auul. Phys. Lett.*, **62**, 585 (1993).
(40) H. J. Zhai, J. Dobler, J. Sauer, and L. S. Wang, *J. Am. Chem. Soc.*, **129**, 13270 (2007).
(41) C. Wang, Z. X. Guo, S. Fu, W. Wu, and D. Zhu, *Prog. Polym. Sci.*, **29**, 1079 (2004).
(42) P. A. C. Quist, T. Martens, J. V. Manca, T. J. Savenije, and L. D. A. Siebbeles, *Sol. Energ. Mater. Sol. Cell.*, **90**, 362 (2006).
(43) S. V. Chasteen, V. Sholin, S. A. Carter, and G. Rumbles, *Sol. Energ. Mater. Sol. Cell.*, **92**, 651 (2008).
(44) G. D. Sharma, P. B. Raju, and M. S. Roy, *Sol. Energ. Mater. Sol.Cell.*, **92**, 261 (2008).
(45) H. Hoppe and N. S. Sariciftci, *J. Mater. Chem.*, **16**, 45 (2006).